Advanced imaging of tau pathology in Alzheimer disease: new perspectives from super resolution microscopy and label-free nanoscopy

Gabriele S. Kaminski Schierle[1] Claire H Michel[1] and Laura Gasparini[2,&]

[1]*Dept. of Chemical Engineering and Biotechnology, Pembroke Street, University of Cambridge, Cambridge CB2 3RA, UK* [2]*Dept. Neuroscience and Brain Technologies, Istituto Italiano di Tecnologia, Via Morego 30, Genova, Italy*

[&]*current address:* Abbvie Deutschland GmbH & Co, Knollstr. 50, 67061 Ludwigshafen, Germany.

Running Title: Advanced imaging of tauopathy

Address correspondence to
GSKS, Tel. +441223334193; email: gsk20@cam.ac.uk
LG, Tel. +39 010 71781; email: laura.gasparini@abbvie.com

Abstract (Max 250)

Alzheimer's disease (AD) is the main cause of dementia in the elderly population. Over 30 million people worldwide are living with dementia and AD prevalence is projected to increase dramatically in the next two decades. In terms of neuropathology, AD is characterized by two major cerebral hallmarks: extracellular β-amyloid (Aβ) plaques and intracellular tau inclusions, which start accumulating in the brain 15-20 years before the onset of symptoms. Within this context, the scientific community worldwide is undertaking a wide research effort to detect AD pathology at its earliest, before symptoms appear. Neuroimaging of Aβ by positron emission tomography (PET) is clinically available and used for AD diagnosis and staging of Aβ pathology. Substantive efforts are ongoing to develop advanced imaging techniques for early detection of tau pathology. Here, we will briefly describe the key features of tau pathology and its heterogeneity across various neurodegenerative diseases bearing cerebral tau inclusions (i.e., tauopathies). We will outline the current status of research on tau-specific PET tracers and their clinical development. Finally, we will discuss the potential application of novel super-resolution and label-free techniques for investigating tau pathology at the experimental level and their potential application for AD diagnosis.

Alzheimer's disease (AD) is the main cause of dementia in the elderly population. It has been estimated that over 30 million people worldwide are living with dementia and AD prevalence is projected to increase dramatically in the next two decades (Hebert and others, 2013). In terms of neuropathology, AD is characterized by two major cerebral hallmarks: extracellular β-amyloid (Aβ) plaques and intracellular tau inclusions, which start accumulating in the brain 15-20 years before the onset of subtle clinical symptoms (Bateman and others, 2012). Within this context, the scientific community worldwide is undertaking a wide research effort to detect AD pathology at its earliest, before symptoms appear. This is of utmost importance given the consensus in the field that medical treatments should be administered at the earliest stages of the disease to maximize their efficacy in ameliorating or slowing down dementia symptoms.

A variety of strategies are currently being tested to identify suitable disease biomarkers for early recognition of pathological hallmarks. Among those, one promising approach is the detection of neuropathological hallmarks by advanced imaging techniques.

Molecular imaging of Aβ through positron emission tomography (PET) has successfully reached clinical stage with the approval of Aβ-specific PET tracers and is a promising modality for early detection of Aβ and AD diagnosis (reviewed in (Adlard and others, 2014)). In fact, a negative Aβ scan substantially decreases the odds of a person having AD and can impact clinical decision making or treatments. In at-risk patients, a positive scan is associated with a three-fold increase of the risk of converting to dementia (Doraiswamy and others, 2014). One main limitation of Aβ imaging by PET is that amyloid plaques by themselves are insufficient for a definite

diagnosis of AD. For this, detection of tau pathology would also be required, which explains the wide interest for developing imaging techniques for early its detection to aid clinical diagnosis. Here, we will briefly describe the key features of tau pathology and its heterogeneity across various neurodegenerative diseases bearing cerebral tau inclusions (i.e., tauopathies). We will outline the current status of research on tau-specific PET tracers and their clinical development. Finally, we will discuss the potential application of novel super-resolution and label-free techniques for investigating tau pathology at the experimental level and their potential application for AD diagnosis.

Tau histopathology

In 1988, seminal studies by Goedert, Wischik and colleagues (Goedert and others, 1988; Wischik and others, 1988a; Wischik and others, 1988b) demonstrated that the microtubule-associated protein tau is the structural component of paired helical filaments (PHF), which are the building blocks of the intracellular tau inclusions first described in the brain of AD patients. Since then, extensive neuropathological evidence has shown the presence of deposits of tau in a variety of neurodegenerative diseases termed tauopathies, including frontotemporal lobe dementia, Pick's disease, corticobasal degeneration and parasupranuclear palsy. This phenomenon was initially thought to be a non-specific event accompanying the neurodegenerative process. However, the identification of mutations in the *tau* gene causative of FTDP-17 has demonstrated that tau and its aggregation have a key role in neurodegeneration and neuronal death (reviewed in (Gasparini and others, 2007).

Tau inclusions manifest with variously shaped deposits that develop both in neurons and glia with distinctive features across tauopathies. The main structures of Alzheimer-type tau pathology are the so-called neurofibrillary tangles (NFTs). NFTs are flame-shaped or globose intraneuronal inclusions stained by silver and affecting neuron perykaria and proximal neurites. Tau deposits also form in distal isolated dendrites (neuropil threads) and in clustered dystrophic neurites (neuritic plaques). NFTs are composed of protein filaments of various structures, including PHF (Kidd, 1963; 1964) and straight filaments (SF). Both PHF and SF from AD are made of abnormally phosphorylated tau protein (Bramblett and others, 1993; Goedert and others, 1992). Tau inclusions have also been shown in glial cells. Coiled bodies and glial threads are inclusions typical of oligodendroglia and they are predominantly found in white matter. Characteristic tau deposits can be found also in astrocytes in the shape of thorned and tuft astrocytes and astrocytic plaques.

Tau pathology progression and spreading

As for Aβ, tau pathology starts to develop many years before clinical symptoms (Bateman and others, 2012). The formation of tau inclusions progresses with a typical anatomical pattern as demonstrated by the seminal neuropathological work of Braak and Braak (1997) that provide the framework for disease severity staging in AD. In presymptomatic stages of the disease (Stage I and II), tau inclusions appear in the entorhinal cortex and hippocampus. During stage III and IV, tau pathology spreads to the occipito-temporal and insular cortices. At this disease stage, only subtle subclinical manifestations occur. In the following stage V-VI, tau inclusions spread throughout the entire cortex (Braak and Braak, 1997). When tau pathology

reached these final stages, AD is fully symptomatic and a definite diagnosis of dementia can be made.

Recent findings indicate that tau pathology spreads in a hierarchical manner among anatomically connected areas (Ahmed and others, 2014; de Calignon and others, 2012; Hyman, 2014). According to the prion-hypothesis, aggregated forms of tau transfer from one cell to the other *in vitro* (Frost and others, 2009a). In fact, tau aggregates are released from the cells of origin and are taken up by neighboring cells, where they seed further filament formation (Frost and Diamond, 2010). Further, recombinant tau fibrils induce aggregation of intracellular full-length tau in cultured cells (Kfoury and others, 2012). In vivo, injection of brain lysate from the P301S tau transgenic model of tauopathy into the brains of mice expressing wild type human tau induces assembly of wild type tau into filaments and spreading of tau pathology across the brain (Clavaguera and others, 2013; Mazzaro and others, 2016). Similar results were obtained with injection of filaments of recombinant human tau, which cause rapid induction of tau inclusions in the site of injection and subsequent propagation of tau pathology to interconnected areas (Iba and others, 2013). Such propagation of tau aggregates throughout the brain does not require the presence of endogenous Tau in the recipient neurons (Wegmann and other, 2015) but is helped by microglia (Asai and others, 2015). The mechanisms underlying the spreading behavior of tau aggregates are still poorly understood. It has been proposed that tau spreading may occur through trans-synaptic movement of tau aggregates (de Calignon and others, 2012). However, the cell endocytic pathway appears also involved in the process of tau aggregation and pathology propagation. In fact, recent studies with super resolution microscopy have uncovered a previously

unrecognized role for extracellular monomeric tau in the transcellular spreading of tau aggregates (Michel and others, 2014).

PET imaging of tau: a promise for the future

Following the successful clinical application of PET imaging for Aβ, substantive efforts are ongoing to develop PET tracers for detecting tau inclusions. However, the peculiar features of tau inclusions pose several hurdles. First of all, tracer specificity and selectivity should take into account two main factors: i) tau inclusions vary in structure (both macro and ultrastructure), post-translational modifications (e.g., phosphorylation, glycation), and location (intra-neuronal vs intra-glial) across different tauopathies; ii) the amount of tau pathology is significantly lower than that of Aβ pathology (Mukaetova-Ladinska and others, 1993; Naslund and others, 2000); and iii) potential binding to protein aggregates occurring in other neurodegenerative diseases may give false positive results. The resolution of these aspects is obviously fundamental to discriminate different neuropathological hallmarks and therefore, different diseases. Second, affinity for the target structure would also contribute to define the specificity and selectivity of PET tracers against tau. Last, biophysical properties, pharmacokinetics and safety matters should be addressed to get optimal entry in the brain and distribution of the tracer in a safe manner. Despite all these difficulties, several molecules have been developed in recent years with enhanced tau binding capabilities and limited or no Aβ detection (reviewed in (Villemagne and others, 2015). Such compounds are still in research/early development stage and will undergo extensive investigation and validation to enter the clinical use in the near future.

Imaging tau pathology: experimental and clinical application of super-resolution microscopy

The advent of optical super-resolution microscopy techniques has led to a paradigm shift in the field of protein misfolding diseases: Using the technique of *direct* Stochastic Optical Reconstruction Microscopy, *d*STORM (Heilemann and others, 2008), it has been possible to image *in vitro* and in cells the morphology of Aβ fibrils with a resolution better than 20 nm (Kaminski Schierle and others, 2011). The technique thus affords a spatial resolution approaching that of atomic force microscopy (AFM) or scanning electron microscopy (SEM) techniques, whilst offering the advantages of specificity and sensitivity that come with all-optical techniques.

Using single-molecule localisation microscopy (SMLM) the presence of polyglutamine aggregates within cells has been demonstrated with molecular resolution (Sahl and others, 2012). In the latter, fibrillary polyglutamine species formed in cells displayed a number of structural similarities to those observed *in vitro* (Duim and others, 2011), which is different to observations made for Aβ using a similar approach (Kaminski Schierle and others, 2011). Moreover, aggregation of human lysozyme, which occurs in case of hereditary amyloidosis linked to specific lysozyme mutations, were observed both *in vitro* and in cells using *d*STORM and showed similar morphological features (Ahn and others, 2012).

These studies led the way to further investigations, such as measurements of amyloid growth (polymerization) using multi-color SMLM approaches as applied to α-synuclein (Pinotsi and others, 2014; Pinotsi and others, 2016; Roberti and others, 2012) or polyglutamine (Duim and others, 2014). Further, two-color SMLM was used to reveal potential mechanisms of propagation of Tau protein by showing the

association of extracellular and endogenous Tau proteins, which are released together into the extracellular medium (Michel and others, 2014). The latter finding highlights the risk associated with increased levels of extracellular Tau, which in AD patients may drive the spreading of tau pathology. Furthermore, another SMLM-based study demonstrated that in cells, the kinetics of aggregation of mutant Aβ is faster than wild type Aβ, revealing the pathological role of mutant Aβ in AD (Esbjorner and others, 2014). Similarly, two-color SMLM was used to observe that Aβ obtained from the soluble fraction of brain extracts of AD patients showed higher seeding capabilities than that extracted from cerebrospinal fluid (Fritschi and others, 2014). The latter study has been the first implementation of super-resolution microscopy toward AD diagnostic: such technique may be valuable for the early onset detection of Tau pathology since in contrast to Aβ, Tau levels in the CSF increase as the disease progresses (Tapiola and others, 2009). A potential ex vivo diagnostic paradigm based on these results with super-resolution imaging is outlined in Figure 1.

Thus far, SMLM techniques have demonstrated an invaluable potential for the study of neurodegenerative diseases, with its molecular resolution and specificity. However, numerous questions remain unanswered, such as, what is the interaction of each amyloid species with the cellular machinery? Which species are responsible for the triggering of cell death? What is the effect of the presence of these fibrillar structures on synaptic transmission? Super-resolution fluorescence techniques are capable to lift the cover on the molecular interactions of these pathologies and thus may pave the way for novel diagnostic assays and therapeutic strategies to prevent these devastating diseases.

Future perspective of label-free imaging of tau pathology imaging

The imaging of tau inclusions in experimental and neuropathological procedures strongly relies on the use of immunohistochemistry and immunofluorescence using a combination of tau-specific antibodies and dyes recognizing the typical cross-β-sheet structure of tau filaments, such as Thioflavin S, Congo red and derivatives like FSB (Figure 2). This approach is informative on the content of tau protein, its post-translational modification (e.g. phosphorylation) and to some extent, cross-β-sheet content of inclusions. However, the differential amount of tau filaments in soma and neurites (the amount in neuritis is extremely low compared to soma – see Figure 2) poses significant challenges to the concomitant imaging of these compartments. Further, current techniques cannot provide information of the dynamics of tau aggregation, nor on the type of aggregate strains contained in the inclusions. The application of label-free spectroscopic principles to the microscopy field will possibly further innovate the imaging of tau pathology in the future. Efforts to apply Raman, infrared (IR) spectroscopy and intrinsic amyloid fluorescence principles are ongoing. Implementing such techniques would add significant information about the chemistry of the sample and/or the presence of specific structural features (e.g., β-sheet conformation of aggregates) and their dynamic structural changes in time. Neither Raman, IR nor intrinsic amyloid fluorescence microscopy has been currently applied to image tau inclusions. However, spectroscopic studies of recombinant tau aggregates provide hints on the potential information we might get from the development of such techniques. Fourier transform IR (FT-IR) spectroscopy has been applied to detect the content of α-helices and cross-β-sheet structure in filaments obtained by the aggregation *in vitro* of human recombinant tau protein or tau

filaments extracted from AD brain samples (Berriman and others, 2003; Sadqi and others, 2002; Schweers and others, 1994). Through FT-IR, it has been also possible to monitor the transition from random-coil to β-sheet structure during the aggregation of recombinant human tau *in vitro*. The spectra obtained by FT-IR spectroscopy show a maximum at 1650 cm^{-1} for the soluble, unfolded tau protein and a shoulder at 1630 cm^{-1} only in samples of aggregated tau protein (von Bergen and others, 2005). Importantly, such a shoulder is also detected in PHF extracted from samples of AD brain (von Bergen and others, 2005) and is consistent with the presence of β-sheet structure in such filaments (Berriman and others, 2003). FT-IR also detects β-sheet content in tau filaments with diverse conformation (Frost and others, 2009b). Likewise, UV Raman Resonance (UVRR) spectroscopy has been applied to investigate the aggregation of recombinant tau *in vitro*, yielding interesting results on the complexity of the dynamic of tau aggregation (Ramachandran and others, 2014). These results indicate that this technique is potentially applicable to the analysis of the variety of tau aggregates conformations associated with different tau lesions. The use of FT-IR spectroscopy principles in combination with probes specific for tau may allow to selectively image tau pathology combining spatial, chemical and conformational details. Within this context, it is noteworthy to mention the possibility to use tau specific antibody fragments labeled with fluorescent near-IR dyes (Krishnaswamy and others, 2014) and efforts to develop pathology-specific probes for near-infrared imaging, such as those developed for Aβ pathology (Schmidt and Pahnke, 2012).

Furthermore, intrinsic fluorescence of amyloids has been applied to study α-synuclein fibril growth in a label-free manner *in vitro* (Pinotsi and others, 2013).

Similar intrinsic fluorescence can be observed in fibrils formed by different variants of recombinant Tau (Figure 3) (Chan and others, 2013; Chan and others, 2014; Michel and others, 2014). The latter has further been successfully applied to develop an amyloid sensor for the study of amyloid aggregation in live cells (Esbjorner and others, 2014; Kaminski and others, 2014; Kaminski Schierle and others, 2011; Kaminski Schierle and others, 2014; Kumar and others, 2014; Michel and others, 2014). Whether or not the intrinsic amyloid fluorescence is amendable to super-resolution microscopy is currently under investigation. One foreseeable problem is discriminating tau intrinsic fluorescence from background fluorescence within tissue.

In conclusion, the development of super resolution microscopy is revolutionizing the imaging paradigms providing unprecedented tools for investigating the pathophysiological mechanisms of AD driven by aggregation of pathological proteins, such as Aβ and tau. The future development of label-free high resolution techniques will further advance our capabilities adding structural information to the qualitative specificity of optical imaging.

Acknowledgments

LG acknowledges funding from the European Community's Seventh Framework Program (FP7/2012-2015) under grant agreement n°280804. GSSK acknowledges funding from the U.K. Medical Research Council (MR/K015850/1 and MR/K02292X/1), Alzheimer's Research UK (ARUK-EG2012A-1), U.K. Engineering and Physical Sciences Research Council (EPSRC) (EP/H018301/1) and the Wellcome Trust (089703/Z/09/Z).

References

Adlard PA, Tran BA, Finkelstein DI, Desmond PM, Johnston LA, Bush AI, Egan GF. 2014. A review of beta-amyloid neuroimaging in Alzheimer's disease. Front Neurosci 8: 327.

Ahmed Z, Cooper J, Murray TK, Garn K, McNaughton E, Clarke H, Parhizkar S, Ward MA, Cavallini A, Jackson S, Bose S, Clavaguera F, Tolnay M, Lavenir I, Goedert M, Hutton ML, O'Neill MJ. 2014. A novel in vivo model of tau propagation with rapid and progressive neurofibrillary tangle pathology: the pattern of spread is determined by connectivity, not proximity. Acta Neuropathol 127(5): 667-83.

Ahn M, De Genst E, Kaminski Schierle GS, Erdelyi M, Kaminski CF, Dobson CM, Kumita JR. 2012. Analysis of the native structure, stability and aggregation of biotinylated human lysozyme. PLoS One 7(11): e50192.

Allen B, Ingram E, Takao M, Smith MJ, Jakes R, Virdee K, Yoshida H, Holzer M, Craxton M, Emson PC, Atzori C, Migheli A, Crowther RA, Ghetti B, Spillantini MG, Goedert M. 2002. Abundant tau filaments and nonapoptotic neurodegeneration in transgenic mice expressing human P301S tau protein. J.Neurosci. 22(21): 9340-9351.

Asai H, Ikezu S, Tsunoda S, Medalla M, Luebke J, Haydar T, Wolozin B, Butovsky O, Kugler S, Ikezu T. 2015. Depletion of microglia and inhibition of exosome synthesis halt tau propagation. Nat Neurosci 18(11): 1584-93.

Barghorn S, Mandelkow E. 2002. Toward a unified scheme for the aggregation of tau into Alzheimer paired helical filaments. Biochemistry 41(50): 14885-14896.

Bateman RJ, Xiong C, Benzinger TL, Fagan AM, Goate A, Fox NC, Marcus DS, Cairns NJ, Xie X, Blazey TM, Holtzman DM, Santacruz A, Buckles V, Oliver A, Moulder K, Aisen PS, Ghetti B, Klunk WE, McDade E, Martins RN, Masters CL, Mayeux R, Ringman JM, Rossor MN, Schofield PR, Sperling RA, Salloway S, Morris JC, Dominantly Inherited Alzheimer N. 2012. Clinical and biomarker changes in dominantly inherited Alzheimer's disease. N Engl J Med 367(9): 795-804.

Berriman J, Serpell LC, Oberg KA, Fink AL, Goedert M, Crowther RA. 2003. Tau filaments from human brain and from in vitro assembly of recombinant protein show cross-beta structure. Proc.Natl.Acad.Sci.U.S.A 100(15): 9034-9038.

Braak H, Braak E. 1997. Staging of Alzheimer-related cortical destruction. Int Psychogeriatr 9 Suppl 1: 257-61; discussion 269-72.

Bramblett GT, Goedert M, Jakes R, Merrick SE, Trojanowski JQ, Lee VM. 1993. Abnormal tau phosphorylation at Ser396 in Alzheimer's disease recapitulates development and contributes to reduced microtubule binding. Neuron 10(6): 1089-1099.

Chan FTS, Kaminski Schierle GS, Kumita JR, Bertoncini CW, Dobson CM, Kaminski CF. 2013. Protein amyloids develop an intrinsic fluorescence signature during aggregation. Analyst 138(7): 2156-2162.

Chan FTS, Pinotsi D, Gabriele S, Schierle K, Kaminski CF. 2014. Chapter 13 - Structure-Specific Intrinsic Fluorescence of Protein Amyloids Used to Study their Kinetics of Aggregation. In: Bio-nanoimaging. Lyubchenko VNUL, editor. Boston: Academic Press. pp 147-155.

Clavaguera F, Akatsu H, Fraser G, Crowther RA, Frank S, Hench J, Probst A, Winkler DT, Reichwald J, Staufenbiel M, Ghetti B, Goedert M, Tolnay M. 2013. Brain homogenates from human tauopathies induce tau inclusions in mouse brain. Proc Natl Acad Sci U S A 110(23): 9535-40.

de Calignon A, Polydoro M, Suarez-Calvet M, William C, Adamowicz DH, Kopeikina KJ, Pitstick R, Sahara N, Ashe KH, Carlson GA, Spires-Jones TL, Hyman BT. 2012. Propagation of tau pathology in a model of early Alzheimer's disease. Neuron 73(4): 685-97.

Doraiswamy PM, Sperling RA, Johnson K, Reiman EM, Wong TZ, Sabbagh MN, Sadowsky CH, Fleisher AS, Carpenter A, Joshi AD, Lu M, Grundman M, Mintun MA, Skovronsky DM, Pontecorvo MJ, Group AAS, Group AAS. 2014. Florbetapir F 18 amyloid PET and 36-month cognitive decline: a prospective multicenter study. Mol Psychiatry 19(9): 1044-51.

Duim WC, Chen B, Frydman J, Moerner WE. 2011. Sub-diffraction imaging of huntingtin protein aggregates by fluorescence blink-microscopy and atomic force microscopy. Chemphyschem 12(13): 2387-90.

Duim WC, Jiang Y, Shen K, Frydman J, Moerner WE. 2014. Super-resolution fluorescence of huntingtin reveals growth of globular species into short fibers and coexistence of distinct aggregates. ACS Chem Biol 9(12): 2767-78.

Esbjorner EK, Chan F, Rees E, Erdelyi M, Luheshi LM, Bertoncini CW, Kaminski CF, Dobson CM, Kaminski Schierle GS. 2014. Direct observations of amyloid beta self-assembly in live cells provide insights into differences in the kinetics of Abeta(1-40) and Abeta(1-42) aggregation. Chem Biol 21(6): 732-42.

Fritschi SK, Langer F, Kaeser SA, Maia LF, Portelius E, Pinotsi D, Kaminski CF, Winkler DT, Maetzler W, Keyvani K, Spitzer P, Wiltfang J, Kaminski Schierle GS, Zetterberg H, Staufenbiel M, Jucker M. 2014. Highly potent soluble amyloid-beta seeds in human Alzheimer brain but not cerebrospinal fluid. Brain 137(Pt 11): 2909-15.

Frost B, Diamond MI. 2010. Prion-like mechanisms in neurodegenerative diseases. Nat Rev Neurosci 11(3): 155-9.

Frost B, Jacks RL, Diamond MI. 2009a. Propagation of tau misfolding from the outside to the inside of a cell. J Biol Chem 284(19): 12845-52.

Frost B, Ollesch J, Wille H, Diamond MI. 2009b. Conformational diversity of wild-type Tau fibrils specified by templated conformation change. J Biol Chem 284(6): 3546-51.

Gasparini L, Crowther RA, Martin KR, Berg N, Coleman M, Goedert M, Spillantini MG. 2011. Tau inclusions in retinal ganglion cells of human P301S tau transgenic mice: Effects on axonal viability. Neurobiology of Aging 32(3): 419-433.

Gasparini L, Terni B, Spillantini MG. 2007. Frontotemporal dementia with tau pathology. Neurodegener.Dis. 4(2-3): 236-253.

Goedert M, Spillantini MG, Cairns NJ, Crowther RA. 1992. Tau proteins of Alzheimer paired helical filaments: abnormal phosphorylation of all six brain isoforms. Neuron 8(1): 159-168.

Goedert M, Wischik CM, Crowther RA, Walker JE, Klug A. 1988. Cloning and sequencing of the cDNA encoding a core protein of the paired helical

filament of Alzheimer disease: identification as the microtubule-associated protein tau. Proc.Natl.Acad.Sci.U.S.A 85(11): 4051-4055.

Hebert LE, Weuve J, Scherr PA, Evans DA. 2013. Alzheimer disease in the United States (2010-2050) estimated using the 2010 census. Neurology 80(19): 1778-83.

Heilemann M, van de Linde S, Schuttpelz M, Kasper R, Seefeldt B, Mukherjee A, Tinnefeld P, Sauer M. 2008. Subdiffraction-resolution fluorescence imaging with conventional fluorescent probes. Angew Chem Int Ed Engl 47(33): 6172-6.

Hyman BT. 2014. Tau Propagation, Different Tau Phenotypes, and Prion-like Properties of Tau. Neuron 82(6): 1189-90.

Iba M, Guo JL, McBride JD, Zhang B, Trojanowski JQ, Lee VM. 2013. Synthetic tau fibrils mediate transmission of neurofibrillary tangles in a transgenic mouse model of Alzheimer's-like tauopathy. J Neurosci 33(3): 1024-37.

Kaminski CF, Pinotsi D, Michel CH, Kaminski Schierle GS. Nanoscale imaging of neurotoxic proteins2014. p 91690N-91690N-10.

Kaminski Schierle GS, Bertoncini CW, Chan FT, van der Goot AT, Schwedler S, Skepper J, Schlachter S, van Ham T, Esposito A, Kumita JR, Nollen EA, Dobson CM, Kaminski CF. 2011. A FRET sensor for non-invasive imaging of amyloid formation in vivo. Chemphyschem 12(3): 673-80.

Kaminski Schierle GS, Sauer M, Kaminski CF. 2014. Chapter 10 - Probing Amyloid Aggregation and Morphology In Situ by Multiparameter Imaging and Super-Resolution Fluorescence Microscopy. In: Bio-nanoimaging. Lyubchenko VNUL, editor. Boston: Academic Press. pp 105-120.

Kfoury N, Holmes BB, Jiang H, Holtzman DM, Diamond MI. 2012. Trans-cellular propagation of Tau aggregation by fibrillar species. J Biol Chem 287(23): 19440-51.

Kidd M. 1963. Paired helical filaments in electron microscopy of Alzheimer's disease. Nature 197: 192-3.

Kidd M. 1964. Alzheimer's Disease--an Electron Microscopical Study. Brain 87: 307-20.

Krishnaswamy S, Lin Y, Rajamohamedsait WJ, Rajamohamedsait HB, Krishnamurthy P, Sigurdsson EM. 2014. Antibody-derived in vivo imaging of tau pathology. J Neurosci 34(50): 16835-50.

Kumar S, Tepper K, Kaniyappan S, Biernat J, Wegmann S, Mandelkow EM, Muller DJ, Mandelkow E. 2014. Stages and conformations of the Tau repeat domain during aggregation and its effect on neuronal toxicity. J Biol Chem 289(29): 20318-32.

Mazzaro N, Barini E, Spillantini MG, Goedert M, Medini P, Gasparini L. 2016. Tau-Driven Neuronal and Neurotrophic Dysfunction in a Mouse Model of Early Tauopathy. J Neurosci 36(7): 2086-100.

Michel CH, Kumar S, Pinotsi D, Tunnacliffe A, St George-Hyslop P, Mandelkow E, Mandelkow EM, Kaminski CF, Kaminski Schierle GS. 2014. Extracellular monomeric tau protein is sufficient to initiate the spread of tau protein pathology. J Biol Chem 289(2): 956-67.

Mukaetova-Ladinska EB, Harrington CR, Roth M, Wischik CM. 1993. Biochemical and anatomical redistribution of tau protein in Alzheimer's disease. Am J Pathol 143(2): 565-78.

Naslund J, Haroutunian V, Mohs R, Davis KL, Davies P, Greengard P, Buxbaum JD. 2000. Correlation between elevated levels of amyloid beta-peptide in the brain and cognitive decline. JAMA 283(12): 1571-7.

Pinotsi D, Buell AK, Dobson CM, Kaminski Schierle GS, Kaminski CF. 2013. A label-free, quantitative assay of amyloid fibril growth based on intrinsic fluorescence. Chembiochem 14(7): 846-50.

Pinotsi D, Buell AK, Galvagnion C, Dobson CM, Kaminski Schierle GS, Kaminski CF. 2014. Direct observation of heterogeneous amyloid fibril growth kinetics via two-color super-resolution microscopy. Nano Lett 14(1): 339-45.

Pinotsi D, Michel CH, Buell AK, Laine RF, Mahou P, Dobson CM, Kaminski CF, Kaminski Schierle GS. 2016. Nanoscopic insights into seeding mechanisms and toxicity of alpha-synuclein species in neurons. Proc Natl Acad Sci U S A.

Ramachandran G, Milan-Garces EA, Udgaonkar JB, Puranik M. 2014. Resonance Raman spectroscopic measurements delineate the structural changes that occur during tau fibril formation. Biochemistry 53(41): 6550-65.

Roberti MJ, Folling J, Celej MS, Bossi M, Jovin TM, Jares-Erijman EA. 2012. Imaging nanometer-sized alpha-synuclein aggregates by superresolution fluorescence localization microscopy. Biophys J 102(7): 1598-607.

Sadqi M, Hernandez F, Pan U, Perez M, Schaeberle MD, Avila J, Munoz V. 2002. Alpha-helix structure in Alzheimer's disease aggregates of tau-protein. Biochemistry 41(22): 7150-5.

Sahl SJ, Weiss LE, Duim WC, Frydman J, Moerner WE. 2012. Cellular inclusion bodies of mutant huntingtin exon 1 obscure small fibrillar aggregate species. Sci Rep 2: 895.

Schmidt A, Pahnke J. 2012. Efficient near-infrared in vivo imaging of amyoid-beta deposits in Alzheimer's disease mouse models. J Alzheimers Dis 30(3): 651-64.

Schweers O, Schonbrunn-Hanebeck E, Marx A, Mandelkow E. 1994. Structural studies of tau protein and Alzheimer paired helical filaments show no evidence for beta-structure. J.Biol.Chem. 269(39): 24290-24297.

Tapiola T, Alafuzoff I, Herukka SK, Parkkinen L, Hartikainen P, Soininen H, Pirttila T. 2009. Cerebrospinal fluid {beta}-amyloid 42 and tau proteins as biomarkers of Alzheimer-type pathologic changes in the brain. Arch Neurol 66(3): 382-9.

Villemagne VL, Fodero-Tavoletti MT, Masters CL, Rowe CC. 2015. Tau imaging: early progress and future directions. Lancet Neurol 14(1): 114-24.

von Bergen M, Barghorn S, Biernat J, Mandelkow EM, Mandelkow E. 2005. Tau aggregation is driven by a transition from random coil to beta sheet structure. Biochim.Biophys.Acta 1739(2-3): 158-166.

Wischik CM, Novak M, Edwards PC, Klug A, Tichelaar W, Crowther RA. 1988a. Structural characterization of the core of the paired helical filament of Alzheimer disease. Proc.Natl.Acad.Sci.U.S.A 85(13): 4884-4888.

Wischik CM, Novak M, Thogersen HC, Edwards PC, Runswick MJ, Jakes R, Walker JE, Milstein C, Roth M, Klug A. 1988b. Isolation of a fragment of tau derived from the core of the paired helical filament of Alzheimer disease. Proc.Natl.Acad.Sci.U.S.A 85(12): 4506-4510.

Figures and legends

Figure 1 – Ex-vivo Screening test for patients with neurodegenerative diseases applying super-resolution microscopy. Patients could be screened for Alzheimer's disease, or other amyloid-caused neurodegenerative disease, with the use of CSF samples. Each patient sample could be divided into fractions, each incubated with an excess amount of labelled monomer of amyloid proteins such as Aβ, Tau, α-synuclein, huntingtin. The presence of seeds in the CSF sample would then be probed by super-resolution imaging of monomer elongation, the frequency of elongated fibrils being correlated with the number of seeds present in the patient's CSF and therefore the stage of the disease.

Figure 2 - Representative maximal projection of confocal z-stack images of one retinal ganglion neuron from the P301S mutant human tau transgenic mouse model of tauopathy (Allen and others, 2002) bearing inclusions of phosphorylated tau filaments containing β-sheet secondary structure. Phosphorylated tau (b; c, green) was visualized by immunostaining with AT8 anti-phospho-tau monoclonal antibodies and aggregates with β-sheet conformation were counterstained using the Congo red analogue FSB (a; c, blue) as previously described (Gasparini and others, 2011). Arrow and arrowheads indicate $FSB^+/AT8^+$ aggregates in soma and dendrites, respectively. Panels d-f images corresponding to squared areas 1 (d), 2 (e) and 3 (f) in a-b representing FSB staining (i panels) and AT8 immunoreactivity (ii panels). Scale bars: 25 μm.

Figure 3 – Tau fibrils display intrinsic fluorescence in the visible range. A: 10 μM recombinant K18Tau protein fragment, which contains the four repeat domain of full

length human Tau (Barghorn and Mandelkow, 2002), was incubated with 10 µM heparin 5000 MW (Fisher Scientific, Loughborough, UK) for 2 days at 37°C in phosphate buffer saline. Fibrils formed were imaged on a Nikon TE inverted microscope with a 100x, 1.49 NA TIRK objective and a 405 nm excitation laser source (Mitsubishi Electronics Corp., Tokyo, Japan). The fluorescence light in the detection path was filtered by a dichroic filter (Semrock multi-edge dichroic Di01-R405/488/561/635-25x36 followed by a FF01-446/523/600/677-25 filter, Semrock, Rochester NY, USA) and was subsequently filtered further using an additional 452/45 band-pass filter (Semrock), before being projected onto an electron-multiplying CCD camera (Andor ixon 887DV, Belfast, Northern Ireland). i) White light image of a cluster of Tau fibrils, ii) Overlay between the white light and fluorescence image and iii) Fluorescence image only. B: Emission spectrum of K18Tau fibrils, measured at 25°C using a TCS SP5 Leica confocal microscope (Leica Microsystems UK Ltd., Milton Keynes, UK). Note, monomeric K18Tau does not display any detectable fluorescence.

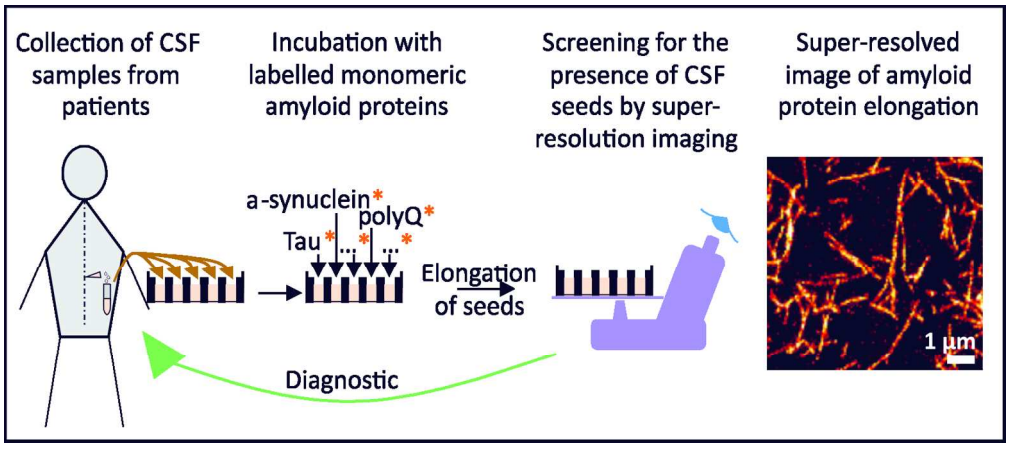

Figure 1 – Ex-vivo Screening test for patients with neurodegenerative diseases applying super-resolution microscopy. Patients could be screened for Alzheimer's disease, or other amyloid-caused neurodegenerative disease, with the use of CSF samples. Each patient sample could be divided into fractions, each incubated with an excess amount of labelled monomer of amyloid proteins such as Aβ, Tau, α-synuclein, huntingtin. The presence of seeds in the CSF sample would then be probed by super-resolution imaging of monomer elongation, the frequency of elongated fibrils being correlated with the number of seeds present in the patient's CSF and therefore the stage of the disease.
145x63mm (300 x 300 DPI)

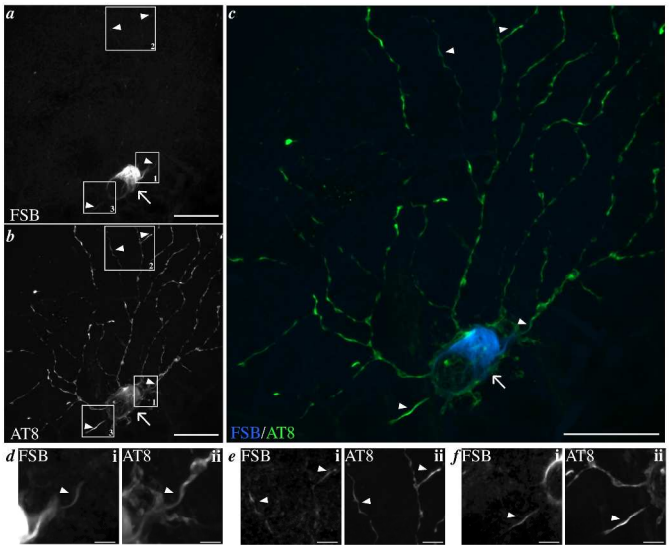

Figure 2 - Representative maximal projection of confocal z-stack images of one retinal ganglion neuron from the P301S mutant human tau transgenic mouse model of tauopathy (Allen and others, 2002) bearing inclusions of phosphorylated tau filaments containing β-sheet secondary structure. Phosphorylated tau (b; c, green) was visualized by immunostaining with AT8 anti-phospho-tau monoclonal antibodies and aggregates with β-sheet conformation were counterstained using the Congo red analogue FSB (a; c, blue) as previously described (Gasparini and others, 2011). Arrow and arrowheads indicate FSB+/AT8+ aggregates in soma and dendrites, respectively. Panels d-f images corresponding to squared areas 1 (d), 2 (e) and 3 (f) in a-b representing FSB staining (i panels) and AT8 immunoreactivity (ii panels). Scale bars: 25 μm.
297x420mm (300 x 300 DPI)

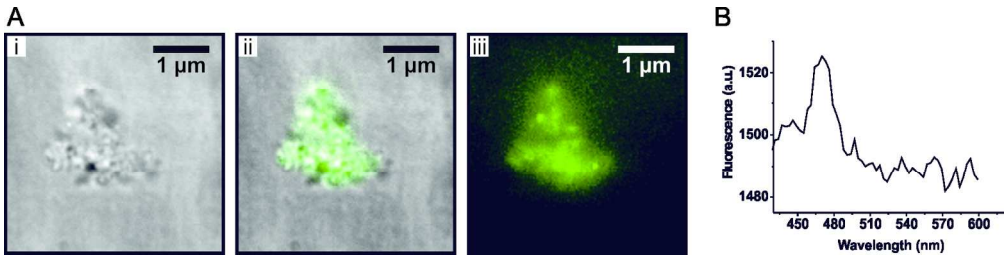

Figure 3 – Tau fibrils display intrinsic fluorescence in the visible range. A: 10 µM recombinant K18Tau protein fragment, which contains the four repeat domain of full length human Tau (Barghorn and Mandelkow, 2002), was incubated with 10 µM heparin 5000 MW (Fisher Scientific, Loughborough, UK) for 2 days at 37°C in phosphate buffer saline. Fibrils formed were imaged on a Nikon TE inverted microscope with a 100x, 1.49 NA TIRK objective and a 405 nm excitation laser source (Mitsubishi Electronics Corp., Tokyo, Japan). The fluorescence light in the detection path was filtered by a dichroic filter (Semrock multi-edge dichroic Di01-R405/488/561/635-25x36 followed by a FF01-446/523/600/677-25 filter, Semrock, Rochester NY, USA) and was subsequently filtered further using an additional 452/45 band-pass filter (Semrock), before being projected onto an electron-multiplying CCD camera (Andor ixon 887DV, Belfast, Northern Ireland). i) White light image of a cluster of Tau fibrils, ii) Overlay between the white light and fluorescence image and iii) Fluorescence image only. B: Emission spectrum of K18Tau fibrils, measured at 25°C using a TCS SP5 Leica confocal microscope (Leica Microsystems UK Ltd., Milton Keynes, UK). Note, monomeric K18Tau does not display any detectable fluorescence.
166x40mm (300 x 300 DPI)